



# Measurement of cross sections for charge pickup by $^{84}\text{Kr}$ on Al, C and $\text{CH}_2$ targets at 400 MeV/u

Rong Li<sup>1</sup> · Dong-Hai Zhang<sup>1</sup>

Received: 19 February 2020 / Revised: 2 April 2020 / Accepted: 2 April 2020 / Published online: 27 May 2020

© China Science Publishing & Media Ltd. (Science Press), Shanghai Institute of Applied Physics, the Chinese Academy of Sciences, Chinese Nuclear Society and Springer Nature Singapore Pte Ltd. 2020

**Abstract** The nuclear charge pickup cross sections of  $^{84}\text{Kr}$  on  $\text{CH}_2$ , C, and Al targets are investigated using CR-39 nuclear track detector at the highest energy of 395 MeV/u. The cross sections for H are calculated from those measured on C and  $\text{CH}_2$  targets. The dependence of the charge pickup cross section on target mass is studied.

**Keywords** Charge pickup reaction · Cross section · CR-39 nuclear track detector

## 1 Introduction

Nuclear charge pickup reactions, which are presumed to be very peripheral interactions in nature, have drawn much attention in heavy ion induced interactions at various energies. The nuclear charge pickup cross sections were first investigated at the Lawrence Berkeley Laboratory Bevalac (LBL) energy [1–9], before being measured at the Brookhaven Alternating Gradient Synchrotron (AGS) energy [10–16], the CERN Super Proton Synchrotron (SPS) energy [17–21], and the GSI Heavy-Ion-Synchrotron (SIS) energy [22–29]. At LBL energy, Ren et al. [7] measured the charge pickup cross sections for 1.7 GeV/u  $^{56}\text{Fe}$ , 1.46 GeV/u  $^{84}\text{Kr}$ , 1.28 GeV/u  $^{139}\text{La}$ , and 0.8 GeV/u  $^{197}\text{Au}$  on a CR-39 target. Combining their results with data

on charge pickup by  $^{12}\text{C}$ ,  $^{18}\text{O}$ , and  $^{20}\text{Ne}$  projectiles [1–5], they found that the cross section for charge pickup by projectiles of order GeV/u is generally given to within a factor of two by the expression  $\sigma_{\Delta Z=+1} = 1.7 \times 10^{-4} \gamma_{\text{PT}} A_{\text{P}}^2$  (in mb). In this expression, the impact parameter  $\gamma_{\text{PT}} = A_{\text{P}}^{1/3} + A_{\text{T}}^{1/3} - 1.0$  implies peripheral collisions, while  $A_{\text{P}}$  and  $A_{\text{T}}$  are the respective projectile and target mass numbers. This steeper projectile mass dependence is not yet to be physically understood for nuclear processes. Since nuclear charge pickup reactions are conjecturally uncommon collisions in nature, the cross sections may be expected to depend on the impact parameter  $\gamma_{\text{PT}} = A_{\text{P}}^{1/3} + A_{\text{T}}^{1/3} - 1.0$ . Moreover, if considered a surface collision, the reactions may also be expected to depend on the cross sectional or surface area and proportional to  $A_{\text{P}}^{2/3}$ . For the dependence of nuclear charge pickup cross section on target mass at LBL energy, a power law relation of  $\sigma_{\Delta Z=+1} = a A_{\text{T}}^b$  was found ( $a$  and  $b$  are fitting parameters), with the exponent  $b$  ranging from 0.2 to 0.45 depending on the type of projectile. Nilsen et al. [10] studied charge pickup reactions with heavy relativistic nuclei at the LBL and AGS energies. To determine the target mass dependence, the power law  $\sigma_{\Delta Z=+1} = a A_{\text{T}}^b$  was fitted against the data, with the fitted exponent  $b$  ranging from  $-0.04$  to  $0.36$  depending on the mass and energy of the projectile. To determine the projectile mass dependence, the power law  $\sigma_{\Delta Z=+1} = a A_{\text{P}}^b$  was fitted to C-target data. A very strong dependence of the form  $A_{\text{P}}^{2.8 \pm 0.1}$  was discovered; for other target data, the same dependence on the projectile mass was found.

This work was supported by the National Natural Science Foundation of China (Nos. 11075100 and 11565001).

✉ Dong-Hai Zhang  
zhangdh@sxnu.edu.cn

<sup>1</sup> Institute of Modern Physics, Shanxi Normal University, Linfen 041004, China

Due to the sparse and sporadic nature of the nuclear charge pickup reactions, these nuclear processes are not well understood. It is clear that the cross sections for charge pickup,  $\sigma_{\Delta Z=+1}$ , are functions of the target and projectile masses, as well as the energy per nucleon of the projectile. It is also probable that there is a dependence on the masses of the produced nuclei. Generally, the nuclear charge pickup cross section decreases with increasing beam energy and increases with projectile and target size.

At energies below the Fermi energy, the mechanism of nuclear charge pickup processes is a transfer reaction where the final states are populated by sequential proton-pickup neutron-stripping processes (or vice versa). When the projectile velocity is smaller than the Fermi velocity of its nucleons, the Fermi spheres of the projectile and target overlap each other at the moment of interaction, such that the proton can jump from the target Fermi sphere into the projectile Fermi sphere. However, the projectile and target Fermi spheres do not overlap at high energies, preventing the transfer of a target proton to the projectile. Instead, we can assume  $\Delta$ -resonance formation and decay in nucleon–nucleon ( $NN$ ) collisions to be the most likely elementary processes in which a projectile neutron can be converted into a proton. At intermediate and high energies, two mechanisms may make a simultaneous contribution to a nuclear charge pickup process, e.g., proton transfer through the nuclear overlap zone, and  $\Delta$ -resonance formation and decay in ( $NN$ ) collisions.

In this paper, the nuclear charge pickup cross sections of  $^{84}\text{Kr}$  on Al, C and  $\text{CH}_2$  targets are studied using a CR-39 nuclear track detector, at the highest energy of 395 MeV/u.

## 2 Experimental details

Three stacks of the sandwiched targets each had a detector–target1–detector–target2–detector arrangement, as shown in Fig. 1. This target–detector configuration was exposed to a 400 MeV/u  $^{84}\text{Kr}$  beam at the Heavy Ion Medical Accelerator in Chiba (HIMAC) facility in the Japanese National Institute of Radiological Sciences (NIRS). The beam fluence was approximately 2000 ions/cm<sup>2</sup>. The detector was a CR-39 nuclear track detector (HARZLAS TD-1, Fukuvi, Japan), with a dimension of  $5.0 \times 5.0 \times 0.08$  cm<sup>3</sup>. The targets were Al with a thickness of 3 mm, C with a thickness of 5 mm, and  $\text{CH}_2$  with a thickness of 10 mm. The beam energy on the upper surface of target 1 was 395 MeV/u for each stack, with variation in the beam energy on the upper surface of target 2 caused by the different target materials. The beam energy on the upper surface of the second Al, C, and  $\text{CH}_2$  targets were 359 MeV/u, 354 MeV/u, and 341 MeV/u, respectively.

CR-39 detectors were etched at the Institute of Modern Physics, Shanxi Normal University, with a 7 N NaOH aqueous etching solution. The etching solution temperature and etching times were 70° and 30 hours, respectively. Tracks from the  $^{84}\text{Kr}$  beam ions and their fragments manifested in the CR-39 sheet as etch-pit cones, on both sides of the CR-39 sheets. The images of the ion tracks were scanned and analyzed automatically by the HSP-1000 microscope system, with the PitFit track measurement software manually checking the images one by one. Approximately  $2.0 \times 10^4$   $^{84}\text{Kr}$  ion tracks were traced from the first CR-39 detector upper surface in the stack to the final CR-39 detector lower surface, using the track tracing method [30]. Details of the methods of track reconstruction, as well as charge identification of beams and their fragment tracks, can be found in our recent publications [31–33] and Ref. [34].

The etching of the CR-39 detector produces conical etch pits coinciding with the penetrating point of the projectile nucleus striking the detector. The area or minor axis of the elliptical etch-pit shape strongly depends on  $Z^*/\beta$  of the projectile and their fragment nucleus, for a detector sensitive range ( $Z^*/\beta > 6$  in this experiment), where  $Z^*$  is the effective charge and  $\beta$  is the velocity of the projectile. For nuclear charge pickup reactions of a projectile on a thin target, the velocity of the projectile fragment can be considered equal to that of the projectile. This relationship is a consequence of a monotonic relation between charge and size or minor axis of the etch-pit, for either the beam nucleus or the nuclear fragment.

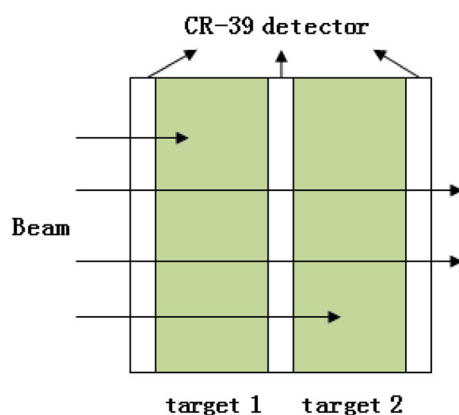


**Fig. 1** (Color online) Sketch of the target–detector configuration exposed to a 400 MeV/u  $^{84}\text{Kr}$  beam

### 3 Results and discussion

When measuring the charge pickup cross sections, the main experimental requirement is to achieve a sufficient charge resolution, to distinguish the relatively rare fragments emerging from the target with an increased charge from the abundant projectile nuclei that pass through the target without changing charge. To achieve this, the reconstructed events matching the possibilities of a  $^{84}\text{Kr}$  projectile passing through the target without changing charge, and a  $^{84}\text{Kr}$  projectile passing through the target forming projectile fragments with an increased charge, were selected for final analysis.

Figure 2 shows the etched track area distribution of beam particles that pass through the target without changing charge and fragments with increased charge for  $^{84}\text{Kr}$  on two Al targets: (a) and (b). For clarity, the interrupted distribution is shown in (c) and (d). A Gaussian fit was applied to the etched track area distribution of surviving beam particles because of the natural Gaussian distribution. The surviving beam particles were determined in the region of four times the standard error to ensure all the surviving beam particles (more than 99.99%) were selected as beam particles. Subsequently, the number of charge pickup events were determined. The same procedure was used for the  $^{84}\text{Kr}$  beam on C and  $\text{CH}_2$  targets. Figures 3 and 4 show the etched track area distributions of beam particles that pass through the target without

changing charge and fragments with increased charge for  $^{84}\text{Kr}$  on C and  $\text{CH}_2$  targets, respectively.

The cross section for a charge pickup reaction is calculated from the equation

$$\sigma_{\Delta Z=+1} = \frac{A_T}{\rho d N_A} \frac{N_{37}}{N_{36}}, \quad (1)$$

where  $A_T$  is the mass number of the target,  $\rho$  is its density,  $d$  is its thickness,  $N_A$  is Avogadro's constant,  $N_{36}$  is the number of beam particles that pass through the target without changing charge, and  $N_{37}$  is the number of charge pickup events observed.

The nuclear charge pickup cross sections for  $^{84}\text{Kr}$  on Al, C, and  $\text{CH}_2$  targets at different energies are calculated and presented in Table 1. The quoted errors are only statistical errors. The cross sections for  $^{84}\text{Kr}$  on H are calculated from the results on C and  $\text{CH}_2$  targets using the relation  $\sigma_H = 0.5(3\sigma_{\text{CH}_2} - \sigma_C)$ . The number of beam particles that pass through the target without changing charge, as well as the number of the fragments with charge  $Z_P + 1 = 37$  (Rb) and  $Z_P + 2 = 38$  (Sr) are also presented in the table. For  $^{84}\text{Kr}$  on an Al target at 395 MeV/u, two fragments with charge  $Z = 38$  are observed, with a nuclear charge pickup cross section of  $4.56 \pm 3.23$  mb. For the same target, the nuclear charge pickup cross section is the same (within experimental error) in our studied beam energy region. We can infer that in our studied energies, these cross sections are dependent on the mass of the target nucleus, increasing as the mass increases.

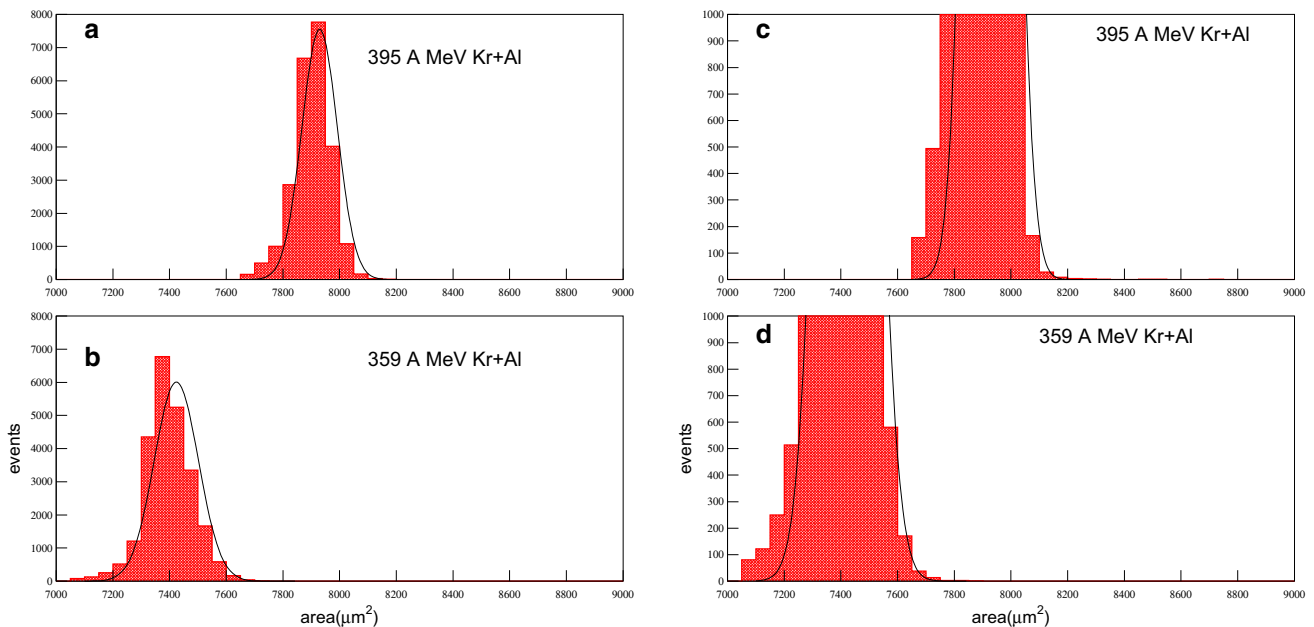


**Fig. 2** (Color online) The etched track area distribution of beam particles that pass through a target without changing charge and fragments with increased charge for a  $^{84}\text{Kr}$  beam on two Al targets (a,

b); c, d are the interrupted distribution of (a, b), respectively. The smooth line is a Gaussian fit

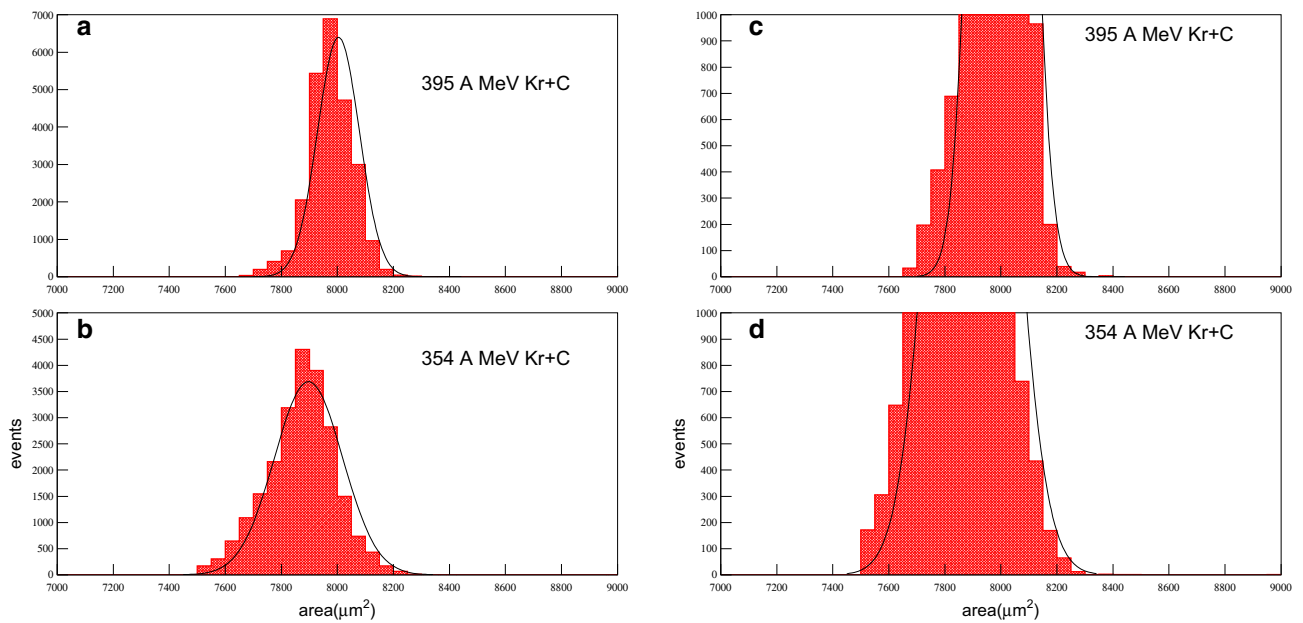


**Fig. 3** (Color online) The etched track area distribution of beam particles that pass through the target without changing charge and fragments with increased charge for a  $^{84}\text{Kr}$  beam on two C targets (a,

b); c, d are the interrupted distribution of (a, b), respectively. The smooth line is a Gaussian fit

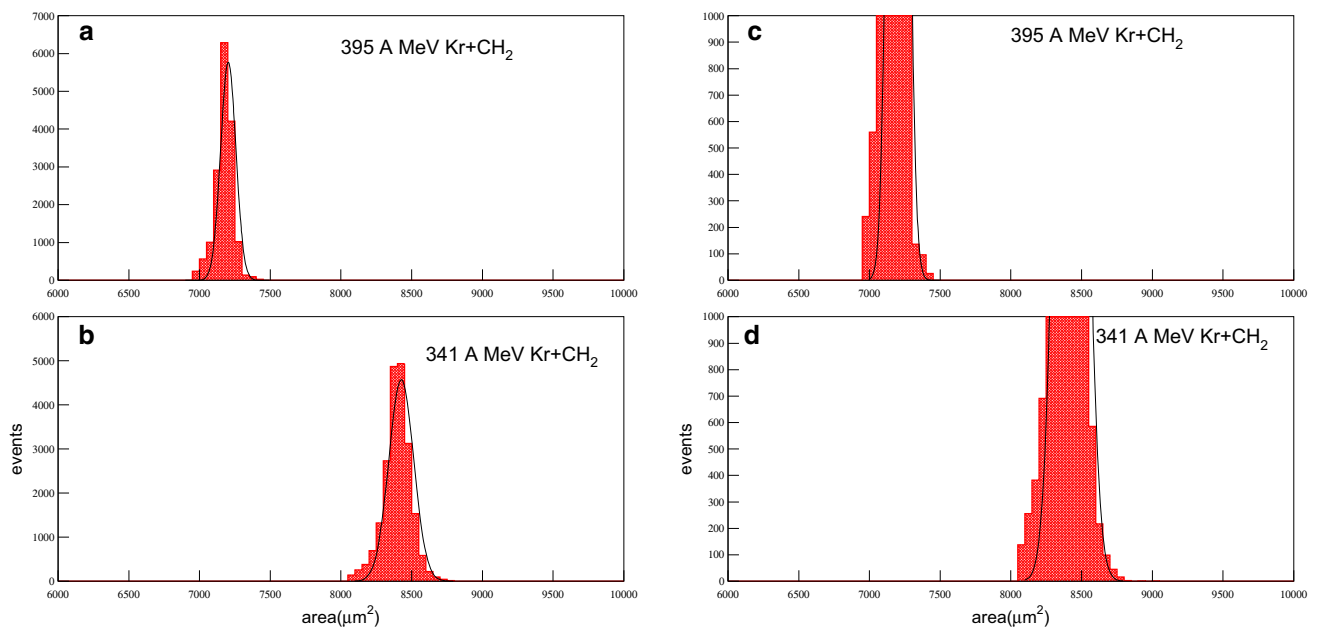


**Fig. 4** (Color online) The etched track area distribution of beam particles that pass through the target without changing charge and fragments with increased charge for a  $^{84}\text{Kr}$  beam on two  $\text{CH}_2$  targets

(a, b); c, d are the interrupted distribution of (a, b), respectively. The smooth line is a Gaussian fit

The study of the correlation between the cross section for heavy ion induced collisions and the target mass has been used to hint about the interaction mechanism. A linear correlation between the cross section and  $A_T$  usually provides insight into the long mean free path of the heavy ion and target. If the nuclear charge pickup cross section is

proportional to  $A_T^{2/3}$ , surface interaction with the target is the assumed interaction mechanism. If the nuclear charge pickup cross section is proportional to  $A_T^{1/3}$ , peripheral interaction with the target is the assumed interaction mechanism.

**Table 1** The charge pickup cross sections, the numbers of surviving beam particles  $^{84}\text{Kr}$ , and the numbers of produced Rb and Sr nuclei in each target at each beam energy

Beam energy (MeV/u)	Target	Thickness of target (mm)	Number of Kr	Number of Rb	Number of Sr	$\sigma_{\Delta Z=+1}$ (mb)
395	Al	2.0	24251	10	2	$22.82 \pm 7.22$
359	Al	2.0	24275	10	0	$22.80 \pm 7.21$
395	C	5.0	24586	4	0	$3.98 \pm 1.99$
354	C	5.0	23276	3	0	$3.15 \pm 1.82$
395	$\text{CH}_2$	10.0	16323	4	0	$2.01 \pm 1.00$
341	$\text{CH}_2$	10.0	20886	5	0	$1.96 \pm 0.88$

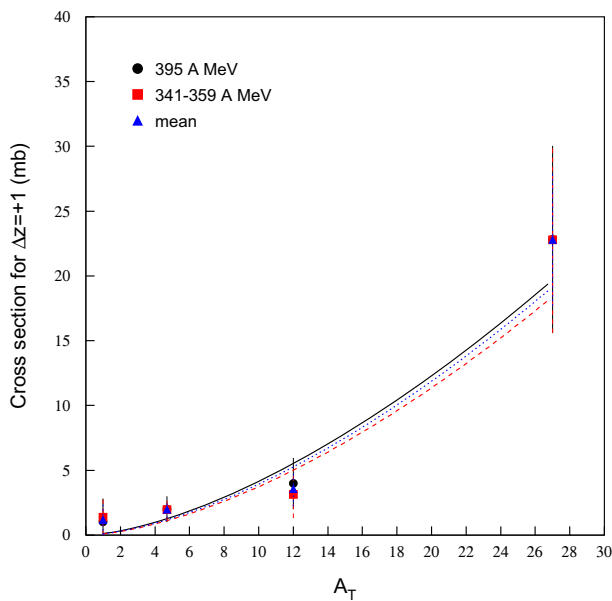
**Fig. 5** (Color online) The nuclear charge pickup cross sections,  $\sigma_{\Delta Z=+1}$ , as a function of target mass number,  $A_T$ , for a  $^{84}\text{Kr}$  projectile

Figure 5 shows the relationship between nuclear charge pickup cross sections and the mass of a target for our studied energies. The data of 395 MeV/u are the cross sections of  $^{84}\text{Kr}$  on the first target, while the data of 341–359 MeV/u are the cross sections of  $^{84}\text{Kr}$  on the second target, with the mean being the average values of the two targets. The experimental data are fitted using a relation

$$\sigma_{\Delta Z=+1} = aA_T^b, \quad (2)$$

where  $a$  and  $b$  are fitting parameters. The fitting parameters  $a$  and  $b$  are presented in Table 2, as well as the minimum  $\chi^2/\text{dof}$ . This strong dependence ( $b \geq 1.0$ ) on target mass is different from results observed for heavier projectiles at higher beam energies [10, 12, 16]. Nilsen et al. [10] investigated the dependence of nuclear charge pickup cross sections on the target mass for 620 MeV/u  $^{84}\text{Kr}$ , discovering different fitting parameters with  $a = 9.59 \pm 0.68\text{mb}$

**Table 2** The fitting parameters  $a$  and  $b$  in Eq. (2) and  $\chi^2/\text{dof}$ 

Beam energy (MeV/u)	$a$	$b$	$\chi^2/\text{dof}$
395	$0.113 \pm 0.433$	$1.566 \pm 1.378$	0.798
341–359	$0.093 \pm 0.369$	$1.604 \pm 1.438$	1.489
Mean	$0.101 \pm 0.278$	$1.592 \pm 0.993$	2.190

and  $b = 0.00 \pm 0.03$ . They also fitted their data using the relation  $\sigma_{\Delta Z=+1} = \alpha + \beta A_T$ , with  $\alpha = 9.52 \pm 0.34$  and  $\beta = 0.014 \pm 0.012$ . This very weak dependence is different from our results and results from other studies [12, 16].

Considering the peripheral collisions property of nuclear charge pickup reactions, the cross sections may be expected to depend on the target mass as  $A_T^{1/3}$ , and being conjecturally a surface collision, may also be expected to depend on the surface area of target as  $A_T^{2/3}$ . Combining these two effects, the nuclear charge pickup reactions should depend on the target mass linearly. The discovery of a power law,  $\sigma_{\Delta Z=+1} = aA_T^b$ , with fitting parameter  $b \sim 1.60$  in our present result confirms the contribution of these two effects, but shows the relationship cannot be explained by these two effects alone.

## 4 Conclusion

The nuclear charge pickup cross sections of a  $^{84}\text{Kr}$  beam on polyethylene, carbon, and aluminum targets are investigated using a CR-39 nuclear track detector, at the highest energy of 395 MeV/u. The cross sections for H are calculated from those measured on C and  $\text{CH}_2$  targets. The dependence of charge pickup cross section on target mass with the relation of  $\sigma_{\Delta Z=+1} = aA_T^b$  is obtained, with the fitting parameter  $b \sim 1.60$ . This strong dependence on target mass confirms that the nuclear charge pickup reaction is



a result of peripheral and surface collisions, but cannot be entirely explained by these two effects alone.

**Acknowledgements** We are grateful to the staff of the HIMAC in NIRS for helping to expose the stacks.

## References

1. D.L. Olson, B.L. Berman, D.E. Greiner et al., Factorization of fragment-production cross sections in relativistic heavy-ion collisions. *Phys. Rev. C* **28**, 1602–1613 (1983). <https://doi.org/10.1103/PhysRevC.28.1602>
2. D.L. Olsen, B.L. Berman, D.E. Greiner et al., Electromagnetic dissociation of relativistic  $^{18}\text{O}$  nuclei. *Phys. Rev. C* **24**, 1529–1539 (1981). <https://doi.org/10.1103/PhysRevC.24.1529>
3. D. Bachelier, J.L. Boyard, T. Hennino et al., First observation of the  $\Delta$  resonance in relativistic heavy-ion charge-exchange reactions. *Phys. Lett. B* **172**, 23–26 (1986). [https://doi.org/10.1016/0370-2693\(86\)90209-1](https://doi.org/10.1016/0370-2693(86)90209-1)
4. M. Roy-Stephan, Excitation of the  $\Delta$  resonance in heavy ion charge exchange reactions. *Nucl. Phys. A* **482**, 373c–382c (1988). [https://doi.org/10.1016/0375-9474\(88\)373C-382C](https://doi.org/10.1016/0375-9474(88)373C-382C)
5. M. Roy-Stephan, Collective excitation of spin-isospin modes. *Nucl. Phys. A* **488**, 187c–201c (1988). [https://doi.org/10.1016/0375-9474\(88\)90261-8](https://doi.org/10.1016/0375-9474(88)90261-8)
6. G. Gerbier, Ren Guoxiao, P.B. Price, Abnormally large momentum loss in charge pickup by 900-MeV/nucleon Au nuclei. *Phys. Rev. Lett.* **60**, 2258–2261 (1988). <https://doi.org/10.1103/PhysRevLett.60.2258>
7. G.X. Ren, P.B. Price, W.T. Williams, Systematics of charge-pickup reactions by GeV/nucleon heavy nuclei. *Phys. Rev. C* **39**, 1351–1358 (1989). <https://doi.org/10.1103/PhysRevC.39.1351>
8. W.R. Binns, J.R. Cummings, T.L. Garrard et al., Charge, mass, and energy changes during fragmentation of relativistic nuclei. *Phys. Rev. C* **39**, 1785–1798 (1989). <https://doi.org/10.1103/PhysRevC.39.1785>
9. A.J. Westphal, Jing Guiru, P.B. Price, Measurement of cross sections for charge pickup by relativistic holmium ions on heavy targets. *Phys. Rev. C* **44**, 1687–1690 (1991). <https://doi.org/10.1103/PhysRevC.44.1687>
10. B.S. Nilsen, C.J. Waddington, W.R. Binns et al., Charge-pickup by heavy relativistic nuclei. *Phys. Rev. C* **50**, 1065–1076 (1994). <https://doi.org/10.1103/PhysRevC.50.1065>
11. C.J. Waddington, W.R. Binns, J.R. Cummings et al., Interactions of 10.6 GeV/n gold nuclei in targets from  $^1\text{H}$  to  $^{82}\text{Pb}$ . *Nucl. Phys. A* **566**, 427c–430c (1994). [https://doi.org/10.1016/0375-9474\(94\)90661-0](https://doi.org/10.1016/0375-9474(94)90661-0)
12. Y.D. He, P.B. Price, Measurement of cross section for charge pickup by 11.4 A GeV gold ions. *Phys. Lett. B* **298**, 50–53 (1993). [https://doi.org/10.1016/0370-2693\(93\)91705-R](https://doi.org/10.1016/0370-2693(93)91705-R)
13. P.B. Price, Y.D. He, Behavior of nuclear projectile fragments produced in collisions of 14.5 A GeV  $^{28}\text{Si}$  with Pb and Cu targets. *Phys. Rev. C* **43**, 835–848 (1991). <https://doi.org/10.1103/PhysRevC.43.835>
14. S.E. Hinzbruch, E. Becker, G. Huntrup et al., Charge-changing interactions of  $^{197}\text{Au}$  at 10 GeV/nucleon in collisions with targets from H to Pb. *Phys. Rev. C* **51**, 2085–2090 (1995). <https://doi.org/10.1103/PhysRevC.51.2085>
15. L.Y. Geer, B.S. Nilsen, C.J. Waddington et al., Charge-changing fragmentation of 10.6 GeV/nucleon  $^{197}\text{Au}$  nuclei. *Phys. Rev. C* **52**, 334–345 (1995). <https://doi.org/10.1103/PhysRevC.52.334>
16. C.J. Waddington, J.R. Cummings, B.S. Nilsen, T.L. Garrard, Fragmentation of relativistic gold by various target nuclei. *Phys. Rev. C* **61**, 024901 (2000). <https://doi.org/10.1103/PhysRevC.61.024901>
17. G. Sher, M.A. Rana, A study of charge-pickup interactions by (158 A GeV) Pb nuclei. *Int. Mod. Phys. E* **20**, 1519–1526 (2011). <https://doi.org/10.1142/S0218301311018459>
18. C. Scheidenberger, I.A. Pshenichnov, T. Aumann et al., Electromagnetically induced nuclear-charge pickup observed in ultrarelativistic Pb collisions. *Phys. Rev. Lett.* **88**, 042301 (2002). <https://doi.org/10.1103/PhysRevLett.88.042301>
19. H. Dekhissi, G. Giacomelli, M. Giorgini et al., Fragmentation studies of 158 A GeV Pb ions using CR39 nuclear track detectors. *Nucl. Phys. A* **662**, 207–216 (2000). [https://doi.org/10.1016/0375-9474\(99\)00414-5](https://doi.org/10.1016/0375-9474(99)00414-5)
20. C. Scheidenberger, I.A. Pshenichnov, K. Summerer et al., Charge-changing interactions of ultrarelativistic Pb nuclei. *Phys. Rev. C* **70**, 014902 (2004). <https://doi.org/10.1103/PhysRevC.70.014902>
21. U.I. Uggerhoj, I.A. Pshenichnov, C. Scheidenberger et al., Charge-changing interactions of ultrarelativistic In nuclei. *Phys. Rev. C* **72**, 057901 (2005). <https://doi.org/10.1103/PhysRevC.72.057901>
22. T. Yamaguchi, T. Ohnishi, T. Suzuki et al., Production cross sections of isotopes formed by fragmentation of  $\sim 1$  A GeV  $^{80}\text{Kr}$  beam. *Phys. Rev. C* **74**, 044608 (2006). <https://doi.org/10.1103/PhysRevC.74.044608>
23. A. Kelic, K.-H. Schmidt, T. Enqvist et al., Isotopic and velocity distributions of  $^{83}\text{Bi}$  produced in charge-pickup reactions of  $^{208}\text{Pb}$  at 1 A GeV. *Phys. Rev. C* **70**, 064608 (2004). <https://doi.org/10.1103/PhysRevC.70.064608>
24. C. Villagrasa-Canton, A. Boudard, J.-E. Ducret et al., Spallation residues in the reaction  $^{56}\text{Fe}+p$  at 0.3 A, 0.5 A, 0.75 A, 1.0 A, and 1.5 A GeV. *Phys. Rev. C* **75**, 044603 (2007). <https://doi.org/10.1103/PhysRevC.75.044603>
25. F. Rejmund, B. Mustapha, P. Armbruster et al., Measurement of isotopic cross sections of spallation residues in 800 A MeV  $^{197}\text{Au}+p$  collisions. *Nucl. Phys. A* **683**, 540–565 (2001). [https://doi.org/10.1016/S0375-9474\(00\)00468-1](https://doi.org/10.1016/S0375-9474(00)00468-1)
26. A. Stolz, T. Faestermann, J. Friese et al., Projectile fragmentation of  $^{112}\text{Sn}$  at  $E_{\text{lab}} = 1$  A GeV. *Phys. Rev. C* **65**, 064603 (2002). <https://doi.org/10.1103/PhysRevC.65.064603>
27. Th Rubehn, R. Bassini, M. Begemann-Blaich et al., Charge pickup of  $^{238}\text{U}$  at relativistic energies. *Phys. Rev. C* **53**, 993–996 (1996). <https://doi.org/10.1103/PhysRevC.53.993>
28. L. Audouin, L. Tassan-Got, P. Armbruster et al., Evaporation residues produced in spallation of  $^{208}\text{Pb}$  by protons at 500 A MeV. *Nucl. Phys. A* **768**, 1–21 (2006). <https://doi.org/10.1016/j.nuclphysa.2006.006>
29. K. Summerer, J. Reinhold, M. Fauerbach et al., Charge-pickup processes in relativistic heavy-ion reactions. *Phys. Rev. C* **52**, 1106–1109 (1995). <https://doi.org/10.1103/PhysRevC.52.1106>
30. S. Ota, S. Kodaira, N. Yasuda et al., Tracking method for the measurement of projectile charge changing cross-section using CR-39 detector with a high speed imaging microscope. *Radiat. Meas.* **43**, S195–S198 (2008). <https://doi.org/10.1016/j.radmeas.2008.04.058>
31. L.-H. Wang, L.-D. Huo, J.-H. Zhu et al., Projectile fragment emission in the fragmentation of  $^{56}\text{Fe}$  on Al, C, and  $\text{CH}_2$  targets. *Nucl. Sci. Tech.* **30**, 186 (2019). <https://doi.org/10.1007/s42365-019-0704-1>
32. L.-D. Huo, L.-H. Wang, J.-H. Zhu et al., The total charge-changing cross sections and the partial cross sections of  $^{56}\text{Fe}$  fragmentation on Al, C, and  $\text{CH}_2$  targets. *Chin. J. Phys.* **60**, 88–97 (2019). <https://doi.org/10.1016/j.cjph.2019.04.022>
33. D.-H. Zhang, R. Shi, J.-S. Li et al., Projectile fragment emission in the fragmentation of  $^{20}\text{Ne}$  on C, Al and  $\text{CH}_2$  targets at 400

- MeV/u. Nucl. Inst. Methods B **435**, 174–179 (2018). <https://doi.org/10.1016/j.nimb.2018.05.045>
34. Y. Zhang, H.-W. Wang, Y.-G. Ma et al., Energy calibration of a CR-39 nuclear-track detector irradiated by charged particles. Nucl. Sci. Tech. **30**, 87 (2019). <https://doi.org/10.1007/s41365-019-0619-x>